Asymmetry in the Autophosphorylation of the Two-Component Regulatory System Transmitter Protein Nitrogen Regulator II of *Escherichia coli*†

Peng Jiang, James A. Peliska, and Alexander J. Ninfa*

Department of Biological Chemistry, University of Michigan Medical School, Ann Arbor, Michigan 48109-0606

Received December 21, 1999; Revised Manuscript Received February 14, 2000

ABSTRACT: Autophosphorylation of the homodimeric two-component system transmitter protein nitrogen regulator II (NRII; also NtrB) of *Escherichia coli* is the first step in the activation of nitrogen-regulated (Ntr) gene transcription. We show that the autophosphorylation of NRII was asymmetric, with phosphorylation of the first and second subunits of the dimer displaying different equilibria (under our experimental conditions $K_1 \sim 0.345$, $K_2 \sim 0.0044$). Phosphorylation of both subunits of NRII was rapid, but the very rapid reversal of the phosphorylation of the second subunit was responsible for the equilibrium position of the reaction. Complete phosphorylation of NRII was only observed under conditions where ADP, a product of the autophosphorylation reaction, was removed by an enzymatic system. Purified, doubly phosphorylated NRII (NRII∼P_2) was stable in the absence of nucleotides at 0 °C but was dephosphorylated to the hemiphosphorylated form at 37 °C. In the presence of a low concentration of ADP, half of the phosphoryl groups from NRII∼P_2 were rapidly dephosphorylated, while the remaining phosphoryl groups were slowly dephosphorylated. Experiments with heterodimers containing wild-type and mutant, nonphosphorylatable subunits suggested that the asymmetry of NRII autophosphorylation was not preexisting but resulted from the autophosphorylation of one subunit.

The two-component signal transduction systems constitute the largest family of related signal transduction systems (for review see refs *1* and *2*). In these systems, the phosphorylation state of a protein known as the "receiver" is used to propagate a signal. The phosphorylation state of the receiver is controlled by one or more "transmitter" proteins, which may act to bring about its phosphorylation or dephosphorylation, and by the accumulation of small phosphorylated metabolic intermediates that can directly phosphorylate the receiver. In addition, unrelated phosphatase enzymes may act to dephosphorylate receiver proteins (*3*). Different two-component systems display different signal sensation mechanisms, and the signal constituted by the phosphorylation of receivers may be translated in a wide variety of ways, including regulation of gene transcription and enzyme activity. In *Escherichia coli* and related bacteria, the transcription of a set of nitrogen-regulated genes known as the Ntr regulon is controlled by the receiver nitrogen regulator I (NRI or NtrC),[1] whose phosphorylation state is controlled by the transmitter nitrogen regulator II (NRII or NtrB; *4*).

The phosphorylation of receiver proteins by transmitter proteins has been examined for several different two-component systems. Transmitter proteins, which are functional only when dimeric (*5*), bind ATP and catalyze the phosphorylation of a conserved histidine residue within the transmitter domain (*6*). [In a small number of exceptions the phosphorylation site is outside of the transmitter domain (*7*).] This autophosphorylation reaction occurs in trans within the dimer; that is, one subunit binds ATP and phosphorylates the other within the dimer (*8*−*10*). For NRII, the trans-intramolecular mechanism was shown to be the exclusive means of autophosphorylation (*10*).

The receiver protein binds the phosphorylated transmitter and catalyzes the transfer of phosphoryl groups from the phosphorylated histidine of the transmitter to a conserved aspartate residue within the receiver domain (*11*, *12*). In the NRI/NRII system and several other systems, the rate of this phosphotransfer reaction is far greater than the rate of transmitter autophosphorylation (*11*, *13*, *14*).

Phosphorylation of the receiver domain is a transient event, owing to the instability of the phosphorylated aspartate moiety. However, several factors render the phosphorylated receiver even more unstable than a typical acyl-phosphate. First, the phosphorylated receivers seem to catalyze their own dephosphorylation, an activity referred to as the autophosphatase activity (*15*). NRI∼P has a modest autophosphatase activity, resulting in a half-life at neutral pH of about 4 min (*11*, *15*). Second, interaction with other proteins may result in the very rapid dephosphorylation of the phosphorylated receiver. In the NRI/NRII system, an additional protein known as PII interacts with NRII and prevents its autophosphoylation (*16*). NRI∼P is rapidly dephosphorylated in the presence of PII and NRII (*4*), an activity referred to as the regulated phosphatase activity of NRII (*15*). Various lines

† This work was supported by Grant GM47460 from the NIH and Grant MCB9318792 from the NSF.

* To whom correspondence should be addressed: Phone 734-763-8065; Fax 734-763-4581; Email aninfa@umich.edu.

[1] Abbreviations: PK, pyruvate kinase; PEP, phosphoenolpyruvate; LDH, lactate dehydrogenase; BSA, bovine serum albumin; NRII, nitrogen regulator II [NtrB, product of *glnL* (*ntrB*)]; NRI, nitrogen regulator I [NtrC, product of *glnG* (*ntrC*)]; PII, signal transduction protein encoded by the *glnB* gene.

10.1021/bi992921w CCC: $19.00
Published on Web 04/07/2000

of evidence suggest that the role of PII is strictly regulatory in this activity, such as the identification of mutant forms of NRII that bring about the dephosphorylation of NRI∼P in the absence of PII (*17*, *18*).

We investigated the stoichiometry of NRII autophosphorylation. For our studies, we took advantage of the small size and convenient behavior of NRII to perform several simple, qualitative assessments of the stoichiometry of NRII autophosphorylation, as well as quantitative assessment of this stoichiometry. Our results indicate that NRII autophosphorylation was asymmetric, due to distinct equilibria for the phosphorylation of the first and second sites in the dimer.

MATERIALS AND METHODS

Purified Proteins. The preparations of NRII, the N-terminal domain of NRI (NRI-N), PII, and NRII-H139N described previously (*14*, *16*, *17*) were used. NRII and NRII-H139N were about 90% pure, as judged by the appearance of the samples after SDS−polyacrylamide gel electrophoresis and staining with Coomassie Brilliant Blue R250 (not shown). The preparations of PII and NRI-N appeared to be homogeneous by similar analysis (not shown). Protein concentrations were determined by the method of Lowry (*19*), with BSA as the standard. The concentrations of NRII and NRII-H139N were calculated from the protein concentration, without accounting for the presence of contaminants. Thus, our calculated concentrations of NRII and NRII-H139N are overestimated by ∼10%. PK and LDH were from Sigma.

Autophosphorylation Reactions. Conditions were 50 mM Tris−Cl, pH 7.5, 10 mM $MgCl_2$, 100 mM KCl, 0.3 or 0.5 mg/mL BSA, as indicated, and ATP, NRII, and temperature as indicated. For quantitative experiments, autophosphorylation reactions containing γ[^{32}P]ATP were used, as previously (*17*). At various times, 4 μL aliquots were spotted onto nitrocellulose filters, immersed in 0.1 M Na_2CO_3 (pH ∼ 11), and washed extensively with Na_2CO_3. Filters were then dried and counted by liquid scintillation. To determine the specific activity of ATP, aliquots of the reaction mixtures were counted directly, without washing, after spotting onto filters.

Coupled Assay System. Reactions were performed and analyzed spectrophotometrically as described previously (*16*). Reaction volume was 350 μL and temperature was 30 °C. Conditions were 50 mM Tris-HCl, pH 7.5, 10 mM $MgCl_2$, 100 mM KCl, 1 mM PEP, 6.9 units of PK, 0.3 M NADH, 23 units of LDH, and indicated concentrations of ATP, NRII, and NRI-N.

Formation of NRII/NRII-H139N Heterodimers and Analysis of Their Autophosphorylation. The urea denaturation/renaturation protocol described previously (*10*) was used in some experiments, as noted. Briefly, NRII and NRII-H139N dimers (1:6.12 ratio) were combined and treated with urea (2.8 M final concentration), incubated for 3 min at 30 °C, and dialyzed against 50 mM Tris-HCl, pH 7.5, and 100 mM KCl. After dialysis, the protein concentration was determined by the method of Lowry (*19*). Autophosphorylation reactions were 50 mM Tris-HCl, pH 7.5, 25 mM $MgCl_2$, 100 mM KCL, 1 mM DTT, 0.3 mg/mL BSA, 0.5 mM ATP, and 1 μM NRII and temperature was 0 °C. The extent of autophosphorylation was determined by liquid scintillation, as described above. Control experiment 1 consisted of NRII alone treated with urea in the presence of an equivalent amount of BSA instead of H139N. Control experiment 2 consisted of mixing NRII and NRII-H139N (1:6.12 ratio) just before adding to the autophosphorylation reaction.

During the course of our studies, we observed that NRII and NRIIH-139N slowly exchange subunits in the absence of urea treatment (unpublished data). We formed heterodimers by incubating NRII and NRII-H139N (1:10 ratio, 3 μM and 30 μM) in 50 mM Tris-HCl, pH 7.5, 10 mM $MgCl_2$, and 100 mM KCl at 37 °C for 3 h. Controls were NRII with an equivalent amount of BSA instead of H139N, and H139N alone. Phosphorylation reactions were as above, with 0.5 mM ATP, 1 μM NRII, and 0.5 mg/mL BSA, at 0 °C. Control experiment 1 was NRII alone; control experiment 2 was NRII and NRII-H139N, which had been incubated alone, combined just before adding to autophosphorylation reactions.

Polyacrylamide Gel Electrophoresis and Thin-Layer Chromatography. Nondenaturing (simple) gel electrophoresis was conducted as described previously (*20*). Urea gel electrophoresis involved the same protocol, except that both stacking and resolving gels contained 6 M urea, and samples were made 4−6 M urea prior to loading. Gels were stained with Coomassie Brilliant Blue R250, destained, dried onto cellophane, and scanned with a desktop scanner to provide the image. Thin-layer chromatography to resolve ATP, ADP, AMP, and P_i was performed as described previously (*21*). A pencil tracing of the nucleotide spots and the autoradiograph was aligned by using three spots of radioactive ink outside of the area of the plate (cropped from the final image), and the composite was scanned with a desktop scanner to provide the image.

Modeling and Simulations. The reaction scheme is as follows:

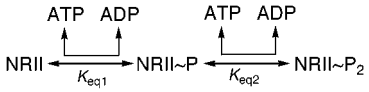

$$K_{eq1} = \frac{[NRII\sim P][ADP]}{[NRII][ATP]}$$

$$K_{eq2} = \frac{[NRII\sim P_2][ADP]}{[NRII\sim P][ATP]}$$

$$[NRII]_0 = [NRII] + [NRII\sim P] + [NRII\sim P_2]$$
$$[ATP]_0 = [ATP] + [ADP]$$
$$[ADP] = [NRII\sim P] + 2\,[NRII\sim P_2].$$

For model 1, where $K_{eq1} \neq K_{eq2}$

$$\frac{1}{K_{eq1}} + K_{eq2} = \frac{2K_{eq2}E_0(S_0)^2}{P^3} + \frac{(E_0S_0) - 4K_{eq2}(E_0S_0) - K_{eq2}(S_0)^2}{P^2} + \frac{2(K_{eq2}S_0) + 2(K_{eq2}E_0) - E_0 - S_0}{P} + 1$$

where $E_0 = [NRII]_0$, $S_0 = [ATP]_0$, and $P = [ADP]$. For model 2, where $K_{eq1} = K_{eq2} = K_{eq}$

$$\frac{2(K_{eq})^2(E_0)(S_0)^2}{P^3} + \frac{(K_{eq}E_0S_0) - 4(K_{eq})^2E_0S_0 - (K_{eq})^2(S_0)^2}{P^2} + \frac{2(K_{eq})^2S_0 + 2(K_{eq})^2E_0 - K_{eq}E_0 - K_{eq}S_0}{P} - (K_{eq})^2 + K_{eq} - 1 = 0$$

Estimation of Equilibrium Constants. Data from experiments conducted at 0 °C was fit by using the equations described above. For model 1, best fit of the data occurred when $K_{eq1} = 0.345$ and $K_{eq2} = 0.00442$. These values were used to plot the solid lines in Figure 2A and Figure 2B.

For model 2, the data could not be fit to the equation (Figure 2, dotted line). The dotted lines shown in Figure 2 represents the predictions of model 2 when $K_{eq} = 0.1$. For the experimental data shown in Figure 2, the ATP concentration was corrected for the amount of ADP in the ATP stock solution. This was determined by use of the PK/LDH coupled enzymatic system described above.

Phosphorylation of NRI-N. Reaction mixtures were as described previously (*16*), contained NRI-N, NRII, ATP, PK, and PEP as indicated, and were incubated at 25 °C. At various times, aliquots were removed and spotted onto nitrocellulose filters, which were immersed and washed extensively in 5% TCA, as described previously (*16*). TCA-precipitable radioactivity was determined by liquid scintillation counting. For experiments where the effect of PII addition on the extent of NRI-N∼P dephosphorylation was determined, reaction mixtures contained NRII (2 μM), NRI-N (1 μM), ATP (0.5 mM), 2-ketoglutarate (30 μM, a ligand of PII that regulates its interaction with NRII), and BSA (0.3 mg/mL), ± PK and PEP as above. Reactions initially lacked PII to permit the phosphorylation of NRI-N. After this phosphorylation had reached equilibrium, PII was added as indicated and the extent of NRI phosphorylation was monitored at various times as above.

RESULTS

Stoichiometry of NRII Autophosphorylation. Our studies of NRII autophosphorylation stoichiometry were motivated by the observation that a different stoichiometry of autophosphorylation was obtained, depending on the assay method. When NRII autophosphorylation was measured in the presence of a coupled enzyme system that regenerates ATP from the ADP formed in the autophosphorylation reaction (*14*, *16*; Materials and Methods), 86% of the sites were phosphorylated within 2 min at 30 °C. Since the NRII proparation used in this study was ∼90% pure, this corresponds to essentially complete phosphorylation of NRII. However, when NRII autophosphorylation was assessed by the incorporation of label from [γ-^{32}P]ATP in experiments where ADP was not removed during the course of the reaction, a smaller fraction of the available sites became autophosphorylated at ATP concentrations well above the apparent K_m (Figure 1, Table 1). Typical results for autophosphorylation reactions conducted at 0 °C and containing 1 mM ATP are shown in Figure 1, as well as the effect of a temperature shift from 0 to 30 °C. The extent of autophosphorylation was dependent on the temperature; with slightly more extensive autophosphorylation seen at 0 °C than at 30 °C (Figure 1 and data not shown). Upon temperature shift, the reaction mixture quickly established a new steady-state level of NRII autophosphorylation (Figure 1 and data not shown). These results indicate that a slightly lower extent of autophosphorylation was obtained when ADP, generated in the autophosphorylation reaction, was not removed. Although the discrepancy between the two assay methods was relatively minor when ATP was 1 mM, it was quite reproducible, and more prominent when lower concentrations of ATP were used (data not shown, see Figure 2).

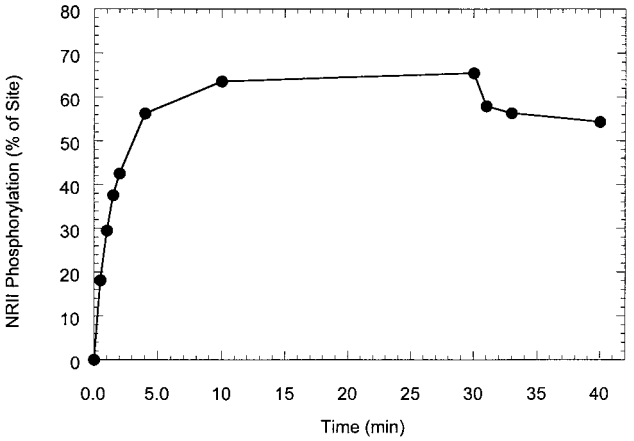

FIGURE 1: Autophosphorylation of NRII and effect of temperature shift. Conditions were as in Materials and Methods; reaction mixtures and contained 5 μM NRII, 1 mM ATP, 0.3 mg/mL BSA, and 1 mM DTT. At the indicated times, aliquots of reaction mixtures were spotted onto nitrocellulose filters, which were washed and counted as in Materials and Methods. The initial reaction temperature was 0 °C, and after 30 min the reaction was shifted to 30 °C.

Table 1: Determination of the ATP K_m for NRII Autophosphorylation

method	[ATP] examined	K_m (μM)	k_{cat}[a] (min^{-1})
coupled assay system[b]	9	18 ± 1	3.88 ± 0.05
filter method[c]	9	31 ± 1.4	1.42 ± 0.03

[a] Per dimer. [b] Determined at 30 °C in the presence of excess NRI-N and 0.6 μM NRII. [c] Direct measurement of NRII autophosphorylation in the absence of NRI-N. NRII was 5 μM and the incubation was at 0 °C.

The autophosphorylation of NRII could be pushed nearly to completion in reaction mixtures where ADP was not removed, by incubation with high concentrations of ATP at 0 °C (Figure 2). The equilibrium extent of autophosphorylation as ATP was varied was not consistent with a mechanism goverened by a single equilibrium constant (Figure 2A, dotted line) but was consistent with a mechanism in which the two subunits of an NRII dimer were phosphorylated with distinct equilibrium constants (Figure 2A, solid line). Our data suggest that the phosphorylation of the first subunit had $K_{eq} \sim 0.35$, and phosphorylation of the second subunit had $K_{eq} \sim 0.0044$ (Figure 2). Similarly, when ADP was added at various concentrations to reaction mixtures where the initial concentration of ATP was fixed, the extent of NRII phosphorylation and the final ratios of ATP/ADP were fit well to a model with distinct equilibrium constants for phosphorylation of the two subunits of the NRII dimer (Figure 2B, solid line) and could not be fit to a model where

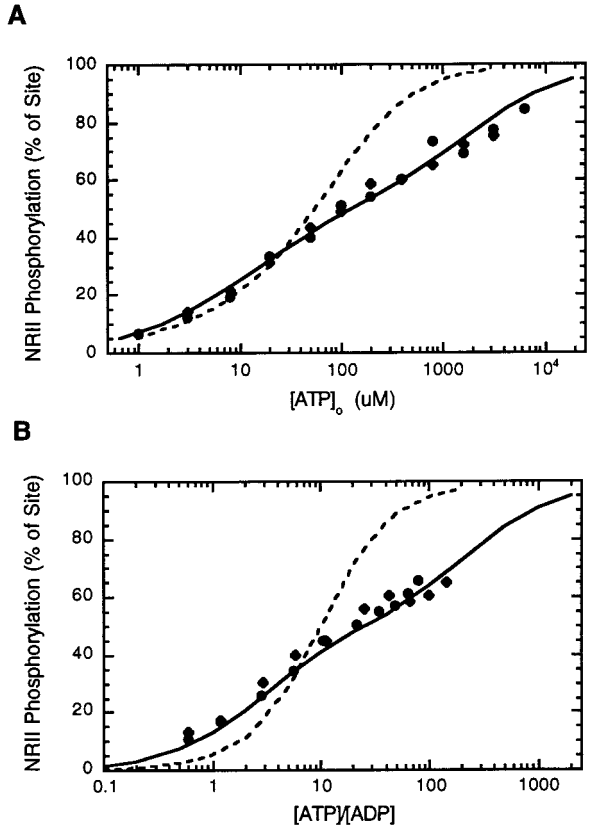

FIGURE 2: Extent of NRII phosphorylation fits a model where phosphorylation of the two subunits of the dimer have distinct equilibria. (A) Phosphorylation at equilibrium with varied $[ATP]_0$. Reactions were as in Materials and Methods, and contained 5 μM NRII and 0.5 mg/mL BSA. Reactions were incubated at 0 °C for 30 min. The solid line is a simulation of model 1 (Materials and Methods), where $K_{eq1} = 0.3389$ and $K_{eq2} = 0.004669$. The dashed line is a simulation using model 2 (Materials and Methods) where $K_{eq} = 0.1$ ● and ◆ are data from two separate experiments. (B) Effect of the ratio [ATP]/[ADP] on the extent of NRII autophosphorylation at equilibrium. Conditions were as in panel A, except that [ADP] was varied from 0 to 5 mM and [ATP] was fixed at 3 mM. The ADP present in the ATP stock solution was estimated by the PK−LDH coupled assay system (Materials and Methods) and used to correct the final [ADP]/[ATP]. The solid line is a simulation with model 1 and $K_{eq1} = 0.35$ and $K_{eq2} = 0.0044$. The dashed line is a simulation with model 2 and $K_{eq} = 0.1$. ● and ◆ are data from two experiments.

a single equilibrium constant described the process (Figure 2B, dotted line).

Determinations of stoichiometry may be subject to errors due to inaccuracy in the estimation of protein concentration, the presence of inactive protein molecules, and inaccuracy in the estimation of the levels of phosphorylation. To qualitatively examine the extent of autophosphorylation of NRII, we examined the mobility of NRII and NRII∼P on nondenaturing polyacrylamide gels and examined the mobility of NRII subunits on denaturing polyacrylamide gels containing urea as the denaturant (in place of the typically used SDS). The nondenaturing gels proved useful for examining the fraction of dimers that were phosphorylated, while the denaturing urea gels, where separation is on the basis of charge as well as mass, proved useful for the estimation of the fraction of NRII subunits that were phosphorylated.

As shown in Figure 3, autophosphorylation of NRII could be monitored by nondenaturing gel electrophoresis, since the

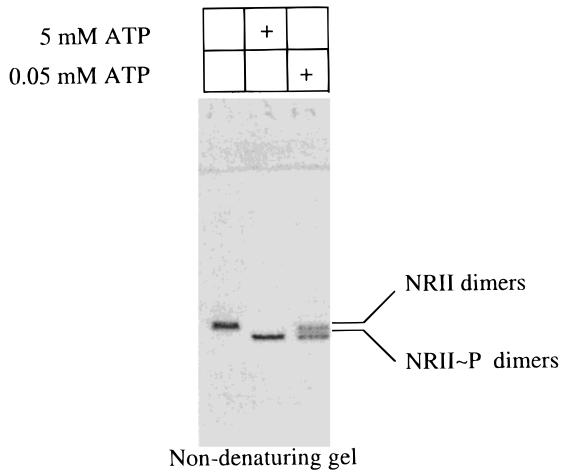

FIGURE 3: Nondenaturing (simple) gel electrophoresis analysis of NRII autophosphorylation. Autophosphorylation reactions containing 1 μM NRII, no BSA, and the indicated ATP concentration were incubated for 20 min at 30 °C, after which EDTA was added to 50 mM to stop the reactions and glycerol was added to 10% (v/v) to facilitate gel loading. The gel was run at 4 °C for 2 h at 150 V in a Bio-Rad minigel apparatus and stained with Commassie Brilliant Blue R-250.

autophosphorylated dimers migrated more rapidly than unphosphorylated NRII dimers. When the low concentration of 0.05 mM ATP was used, NRII was partially phosphorylated, leading to two discrete bands upon electrophoresis, while at 5 mM ATP, only the band corresponding to NRII∼P was observed (Figure 3). In additional experiments using [γ-^{32}P]ATP, it was observed that only the faster-migrating species observed on nondenaturing gels was phosphorylated (E. S. Kamberov and A.J.N., unpublished data). Since (qualitatively) all of the NRII could be converted to NRII∼P, these results exclude the possibility that a significant fraction of our NRII protein preparation was inactive (Figure 3). Similar results were obtained with several other preparations of NRII (data not shown).

The extent of NRII autophosphorylation could also be assessed on denaturing urea-containing gels, where phosphorylated subunits migrated more rapidly than did unphosphorylated subunits (Figure 4). Under conditions where ∼50% of the sites were phosphorylated in quantitative experiments (Figure 2) and where qualitatively all of the NRII migrated as the phosphorylated species on nondenaturing gels (Figure 3), about 50% of the NRII subunits appeared to be phosphorylated on urea-containing gels (Figure 4 and data not shown). Thus, under certain reaction conditions, essentially all of the NRII dimers became phosphorylated on a single subunit, that is, became hemiphosphorylated. The internal consistency of these results suggested that our determination of protein concentration by the method of Lowry was accurate.

Autophosphorylation of NRII in Heterodimers with NRII-H139N Subunits. Another way to qualitatively examine the stoichiometry of NRII autophosphorylation is to examine the effect of forming heterodimers with wild-type NRII subunits and mutant subunits containing the nonphosphorylatable H139N alteration at the site of autophosphorylation. We previously showed that the autophosphorylation of NRII proceeds exclusively by a trans-intramolecular mechanism, in which ATP bound to one subunit is used to phosphorylate the target H139 residue on the other subunit (*10*). Also,

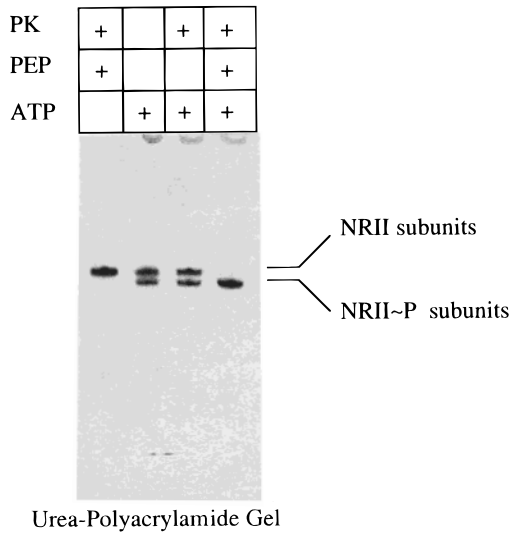

FIGURE 4: Urea gel electrophoretic analysis of NRII autophosphorylation. Autophosphorylation reactions containing 5 μM NRII, no BSA, PK at 0.02 unit/μL, where indicated, PEP at 1 mM, where indicated, and 0.1 mM ATP were incubated for 30 min at 25 °C, after which urea was added to a final concentration of 6 M to stop the reactions and facilitate gel loading. The gel was run at 4 °C for 2 h at 200 V and stained with Coomassie Brilliant Blue R-250.

H139N subunits, while unable to become autophosphorylated, can phosphorylate their partner in heterodimers if that partner has a wild-type site of autophosphorylation (*10*). As before, we formed NRII/NRII-H139N heterodimers from mixtures of the wild-type and mutant proteins, by treatment with a low concentration of urea followed by dialysis to remove the urea (*10*). Additionally, in the course of our work we observed that NRII subunits underwent slow dynamic exchange in solution, leading to spontaneous heterodimer formation over a period of about 2−3 h (P. Jiang et al., manuscript in preparation). Thus, we had two methods for forming heterodimers between NRII and NRII-H139N subunits (mixing and waiting; mixing, urea treatment, and dialysis). Previous and unpublished experiments suggested that subunits exchanged similarly, such that the distribution of subunits into various species reflected the simple proportion of those subunits in the mixture (*10*). Thus, for example, by mixing NRII and NRII-H139N subunits in a 1:10 ratio, ~90% of the wild-type subunits should be distributed into heterodimers with an NRII-H139N subunit.

The ability to form heterodimers of NRII and NRII-H139N subunits permitted us to address the issue of the extent of autophosphorylation in wild-type NRII dimers under those conditions where the reaction seemed to result in hemiphosphorylation of NRII. If this extent was really 100% of the available sites (for example, if the Lowry determination of protein concentration was not accurate), then the presence of a huge excess of NRII-H139N subunits could not increase the extent of NRII autophosphorylation. On the other hand, if NRII~P consisted of an equal mixture of phosphorylated and unphosphorylated subunits (i.e., if the single species obseved on nondenaturing gels was the hemiphosphorylated form), then redistribution of these wild-type subunits into heterodimers with NRII-H139N subunits may increase the extent of their autophosphorylation. Specifically, if there was asymmetry of autophosphorylation, and if this asymmetry was solely due to autophosphorylation itself, then we expect

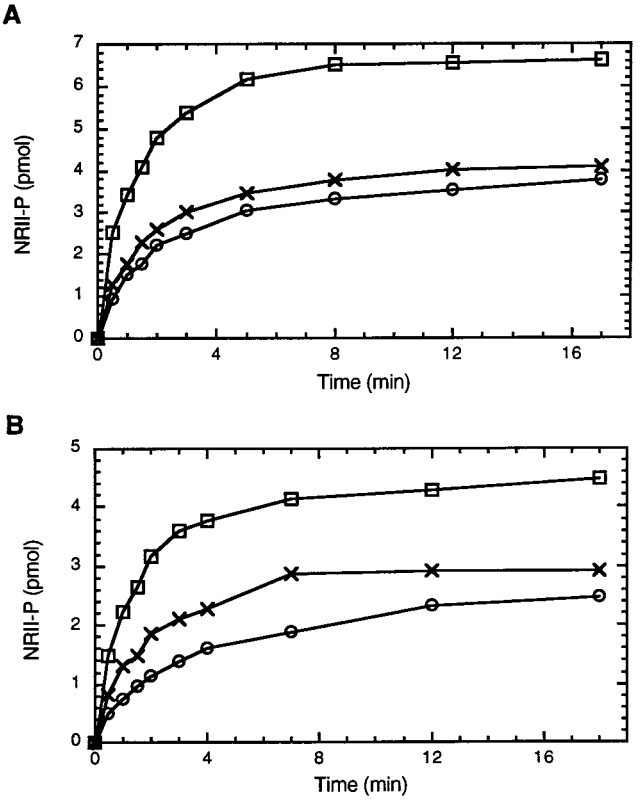

FIGURE 5: Autophosphorylation of NRII subunits when present in heterodimers with H139N subunits. (A) Heterodimers formed by coincubation of NRII and NRII-H139N. NRII was incubated with BSA (○) or with a 10-fold excess of NRII-H139N (□) for 3 h at 37 °C. Autophosphorylation reactions contained 0.5 mM [γ-^{32}P]ATP and were incubated at 0 °C for the indicated times, after which samples were removed, spotted onto nitrocellulose filters, and analyzed as in Materials and Methods. All reactions contained 1 μM NRII. The reactions indicated × contained 1 μM NRII and 10 μM NRII-H139N mixed immediately before adding to the autophosphorylation reaction. The percentage of sites and relative yield for the three autophosphorylation reactions is as follows: (○) 47.4%, 1.0; (×) 51.3%, 1.08; □ 82.9%, 1.75. (B) Heterodimers formed by urea treatment and dialysis of protein mixtures. NRII and NRII-H139N in a 1:6.12 ratio (□), NRII with an equivalent amount of BSA (○), and NRII-H139N in isolation were subjected to the urea/dialysis protocol. After dialysis, the NRII-H139N sample was combined with the NRII sample (6.12 to 1 molar ratio) to constitute the samples designated with ×. Autophosphorylation reactions contained 0.5 mM [γ-^{32}P]ATP and were incubated at 0 °C for the indicated times, after which samples were removed, spotted onto nitrocellulose filters, and analyzed as in Materials and Methods. All reactions contained 1 μM NRII. The percentage of sites and relative yield for the three reactions is as follows: (○), 31.0%, 1.0; (×), 36.6%, 1.18; (□), 56.1%, 1.8. Extent of autophosphorylation in panel B is lower than in panel A because the urea/dialysis method results in some loss of activity.

a doubling of the extent of NRII autophosphorylation when all of the wild-type subunits are distributed into heterodimers with NRII-H139N subunits.

In one experiment, heterodimers were formed by mixing the two proteins and incubating for 3 h at 37 °C, while in a second experiment, heterodimers were formed by subjecting the mixture of proteins to the urea denaturation and dialysis protocol (Materials and Methods). In both experiments, the extent of NRII phosphorylation was approximately doubled by the distribution of most of the wild-type subunits into heterodimers with H139N subunits (Figure 5). These observations suggest that, in wild-type NRII homodimers, only

about half of the available sites were autophosphorylated at equilibrium under the conditions used and that (qualitatively) all of the sites were able to become autophosphorylated when present in heterodimers with H139N subunits (Figure 5). Thus, NRII was hemiphosphorylated, unless very high concentrations of ATP were present (Figure 2) or ADP was removed by a coupled enzymatic system.

Stoichiometry of NRII Autophosphorylation in the Presence of an Enzymatic System for the Removal of ADP. We noted above that nearly complete autophosphorylation of NRII was obtained when NRII autophosphorylation was measured spectrophotometrically by coupling to the PK and LDH reactions (>86% of sites phosphorylated within 2 min at 30 °C). Nearly complete autophosphorylation of both sites in NRII was also obtained when ADP was enzymatically removed from reaction mixtures by the inclusion of pyruvate kinase and its substrate, phospho*enol*pyruvate, in the absence of LDH and NADH. Urea gel analysis showed that when ATP was 0.1 mM, such inclusion shifted the extent of NRII autophosphorylation from ~50% to nearly complete autophosphorylation (Figure 4). Control experiments indicated that neither PK alone (Figure 4) nor PEP alone (not shown) could stimulate the phosphorylation of NRII when added separately at these concentrations. These results, along with the results from the autophosphorylation measurements by coupling to NADH oxidation, suggested that the presence of a very low concentration of ADP, generated in the autophosphorylation reaction, prevented the phosphorylation of the second subunit of NRII dimers.

Stability of Doubly Phosphorylated NRII Dimers. Doubly phosphorylated NRII dimers were prepared in the presence of PK and PEP and separated from low molecular mass reaction components by gel-filtration chromatography (Materials and Methods). These dimers were used to assess the stability of the phosphoryl groups in the doubly phosphorylated dimer. In the absence of added nucleotides, the doubly phosphorylated dimers were stable at 0 °C but decayed slowly at 37 °C such that ~50% of the subunits were phosphorylated after 90 min, as assessed by urea gel electrophoresis (Figure 6). Upon addition of excess ADP and Mg^{2+}, NRII was completely dephosphorylated at both 37 and 0 °C, as assessed by urea gel electrophoresis (not shown). Similarly, addition of excess N-terminal domain of NRI (NRI-N) resulted in the complete dephosphorylation of NRII~P_2, as determined by urea gel analysis (not shown).

Doubly phosphorylated NRII dimers labeled with ^{32}P were formed by use of [γ-^{32}P]ATP to phosphorylate NRII in the presence of PK and PEP and purified by gel filtration chromatography. Urea gel analysis of our doubly phosphorylated NRII~$^{32}P_2$ preparation suggested that it was >90% phosphorylated (not shown), similar to the nonradioactive sample shown in Figure 6. The stability of NRII~^{32}P was assessed at 25 °C in the absence of ATP or upon addition of ATP at various concentrations (Figure 7). The ATP used in these experiments was rendered free of ADP by preincubation with PK and PEP. When PK and PEP were present in the final reaction mixtures to remove ADP, NRII~^{32}P was stable in the presence of ATP (Figure 7A). However, when ADP was allowed to accumulate, addition of ATP to NRII~^{32}P resulted in the rapid turnover of phosphoryl groups from NRII~^{32}P. ATP at the low concentration of 20 μM caused a greater destabilization of NRII~^{32}P than did ATP

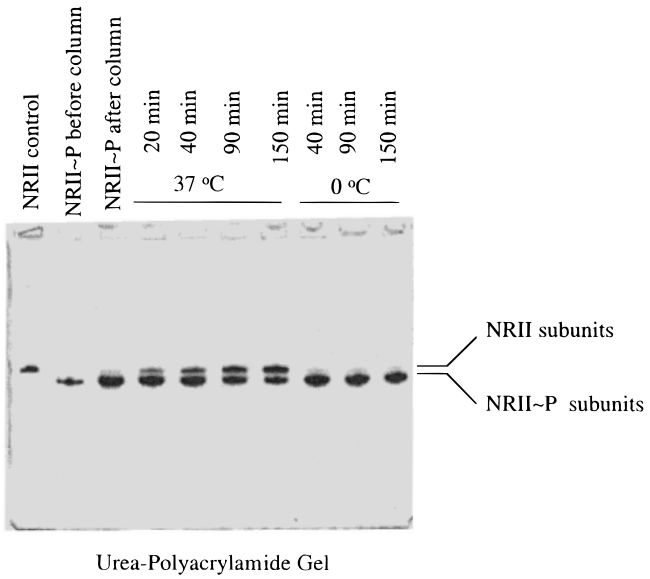

FIGURE 6: Urea gel analysis of the stability of doubly phosphorylated NRII dimers. Doubly phosphorylated NRII dimers were prepared in the presence of 0.5 mM ATP, 0.02 unit/μL PK, and 1 mM PEP and the autophosphorylation reaction mixture was subjected to gel filtration at 4 °C on a 12 mL Sephadex G-25 column in 50 mM Tris-HCl, pH 7.5, 200 mM KCl, 1 mM DTT, and 10% (v/v) glycerol. The peak fraction containing NRII~P_2 was incubated at the indicated temperature for the indicated times, after which urea was added to 6 M final concentration to stop the reactions. The electrophoresis protocol was as described for Figure 4.

at the high concentration of 2 mM (Figure 7B). Phosphoryl groups from NRII~^{32}P appeared in ATP and did not appear in P_i, in these experiments, as revealed by thin-layer chromatography (Figure 7C). Since the ATP used in these experiments was rendered free of ADP, these results suggest that ADP generated upon the phosphorylation of a small number of unmodified sites in our doubly phosphorylated NRII~^{32}P preparation was sufficient to bring about the rapid exchange of isotope from NRII~^{32}P.

The kinetics of dephosphorylation of NRII~^{32}P was examined in the presence of ADP at 20 μM and 100 μM (Figure 8). As shown, approximately 50% of the phosphoryl groups were rapidly turned over, while the remaining phosphoryl groups were slowly turned over. Thus, the dephosphorylation of NRII~^{32}P by ADP was also asymmetric.

Effect of PII on the Extent of NRII Autophosphorylation. Previous studies have shown that the PII protein regulates the extent of NRI phosphorylation by inhibiting the rate of NRII autophosphorylation and by activating the dephosphorylation of NRI~P by NRII. We examined the effect of PII on the rate and extent of NRII autophosphorylation in reaction mixtures containing or lacking PK and PEP (Figure 9). These reaction mixtures also contained BSA at 0.5 mg/mL (to quench nonspecific effects due to slightly different protein concentration) and 2-ketoglutarate, which allosterically regulates the binding of PII to NRII. Control experiments indicated that BSA and 2-ketoglutarate at these concentrations had no effect on the extent of NRII autophosphorylation in the absence of PII (not shown).

In the absence of PK and PEP, PII inhibited the rate of NRII autophosphorylation, as described previously (*16*) but

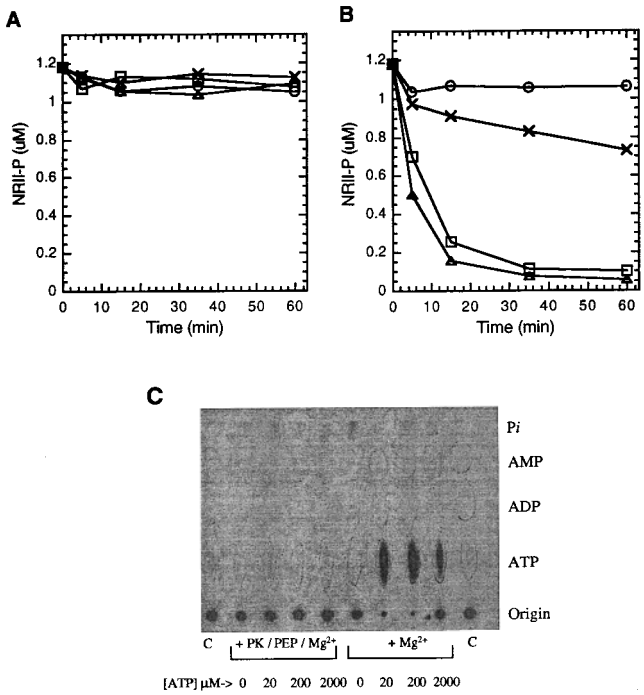

FIGURE 7: Stability of NRII∼P in the presence of ATP. Doubly phosphorylated NRII∼P was formed and purified by gel filtration as described for Figure 6, except that [γ-^{32}P]ATP was used. The unlabeled ATP used to dilute the radioactive stock solution was rendered free from ADP by pretreatment in the following reaction mixture for 10 min at 25 °C: 50 mM ATP, 50 mM Tris-HCl, pH 7.5, 10 mM $MgCl_2$, 100 mM KCl, 0.02 unit/μL PK, and 3 mM PEP. NRII∼P was incubated at 25 °C with conditions as follows: 10 mM $MgCl_2$, 50 mM Tris-HCl, pH 7.5, and 184 mM KCl. Symbols: (○), NRII∼P alone; (□), NRII∼P + 20 μM ATP; (△), NRII∼P + 200 μM ATP; (×), NRII∼P + 2 mM ATP. (A) Incubation as above and containing in addition 0.02 unit/μL PK and 1 mM PEP. (B) Incubation in the absence of PK and PEP. For panels A and B, samples were removed at the indicated times, spotted onto filters, and analyzed as in Materials and Methods. (C) Thin-layer chromatography analysis of the 60 min samples from the experiments shown in panels A and B. Samples were brought to 0.9% SDS to stop the reactions and spotted along with with a carrier containing unlabeled AMP, ADP, and ATP. In the orientation shown, migration was from bottom to top. After chromatography, a pencil tracing of the nucleotide spots was made while the plate was illuminated with a UV lamp. Autoradiography was performed, and the aligned X-ray film and pencil tracing are shown. Samples designated C contained the NRII∼P_2 preparation control (samples stored on ice).

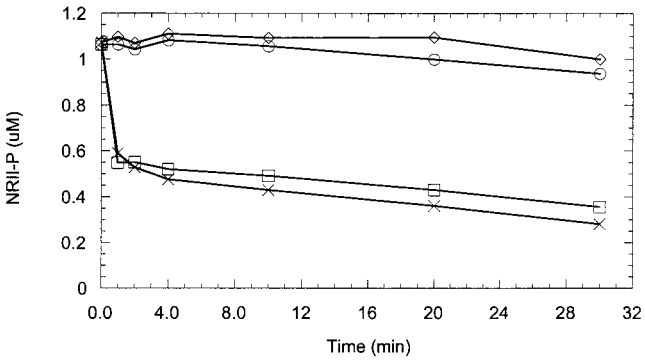

FIGURE 8: Dephosphorylation of NRII∼$^{32}P_2$ by ADP. Reaction conditions were as for the autophosphorylation of NRII, except that ATP was omitted and NRII∼$^{32}P_2$ was used in place of NRII. Reaction mixtures contained NRII∼$^{32}P_2$ (1.1 μM), 2-ketoglutarate (0.03 mM), and BSA (0.5 mg/mL); the incubation temperature was 0 °C. At time 0, reactions were initiated by addition of the following (to the final concentations indicated): (○, ◇) no addition; (□) 100 uM ADP; (×) 20 μM ADP. Two controls are shown because the data for 100 μM ADP and 20 μM ADP were performed in separate experiments using the same NRII∼P_2 preparation.

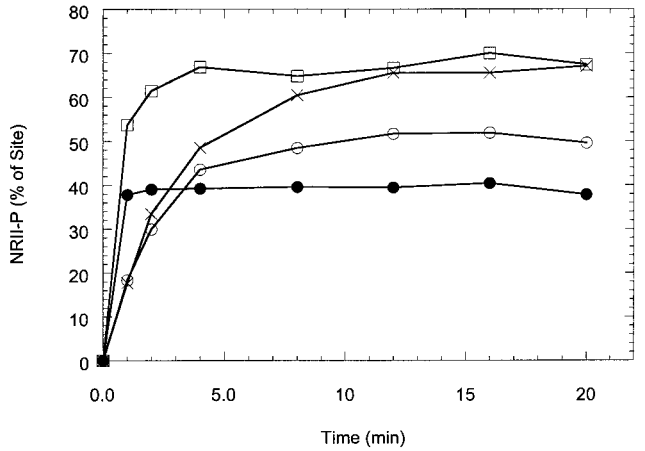

FIGURE 9: Effect of PK, PEP, and PII on the extent and rate of NRII autophosphorylation. Reaction mixtures contained NRII (2 μM), [γ-^{32}P]ATP (0.05 mM), 2-ketoglutarate (0.03 mM), and BSA (0.5 mg/mL). Where indicated, PII was present at 12 μM, PK was 0.02 unit/μL, and PEP was 1 mM. Incubation was at 25 °C. Symbols: (●) no PII, PK, or PEP; (○) PII present; (□) PK and PEP present; (×) PII, PK, and PEP present.

increased the extent of NRII autophosphorylation (Figure 9). Although PII provided only ∼10% increase in the extent of NRII autophosphorylation, this effect was quite reproducible (data not shown). This effect of PII was most pronounced at concentration of ATP where the extent of NRII phosphorylation was less than 50% of the available sites (Figure 9 and data not shown). In the presence of PK and PEP, PII inhibited the rate of NRII autophosphorylation, but eventually the same equilibrium extent of NRII autophosphorylation was obtained as in the presence of PK and PEP and absence of PII (Figure 9).

Effect of ADP on the Extent of Phosphorylation of NRI-N. We examined the extent of NRI-N phosphorylation in the presence and absence of PK and PEP under conditions where NRII was present in excess or limiting concentration. Regardless of whether NRII was limiting or in excess, the presence of PK and PEP had little effect on the rate or extent of NRI-N phosphorylation for the first 20 min of the phosphorylation reactions (data not shown). Therefore, the levels of ADP produced in the reaction mixtures during this time apparently did not significantly affect the phosphorylation of NRI-N. However, addition of ADP to physiological levels to reaction mixtures containing ATP, NRII, and NRI-N caused a significant reduction in the equilibrium extent of NRI-N phosphorylation, regardless of whether NRII was limiting or in excess (Figure 10).

Effect of PK and PEP on the Activation of the Phosphatase Activity of NRII by PII. We examined the effect of adding PII to reaction mixtures containing excess NRII, in which the phosphorylation of NRI-N had been allowed to proceed for 20 min, as in Figure 9 (Materials and Methods). PII brought about the rapid dephosphorylation of NRI-N regardless of whether PK and PEP were present (data not shown). PII was slightly more effective in bringing about the dephosphorylation of NRI-N in the presence of PK and PEP (not shown).

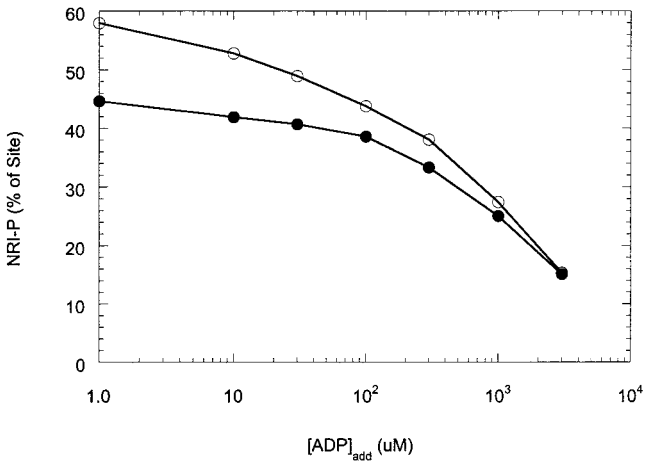

FIGURE 10: Effect of ADP on the extent of NRI-N phosphorylation by NRII. Reaction mixtures contained [γ-^{32}P]ATP (0.5 mM), ADP as indicated, and either 1 μM NRI-N and 2 μM NRII (○) or 15 μM NRI-N and 1 μM NRII (●). Reactions were incubated at 25 °C for 35 min. The data points plotted on the *y*-axis contained no added ADP (plotted as 1 μM to permit use of a log scale on the *x*-axis).

DISCUSSION

Autophosphorylation of the dimeric NRII was asymmetric, due to different equilibria for the two phosphorylation reaction steps. This conclusion, drawn from the data in Figure 2 where the stoichiometry of NRII autophosphorylation was assessed at different concentrations of ATP and at different ATP/ADP ratios, was strengthened by our observation of a dramatic increase in the stoichiometry of NRII autophosphorylation from about half of the available sites to essentially all of the sites when ADP was removed from reaction mixtures by an enzymatic system (Figure 4). Also, the dephosphorylation of NRII∼P_2 by ADP was asymmetric (Figure 8). One possible explanation for these results is that NRII undergoes a concerted conformational change upon autophosphorylation of one subunit. This conformational change may favor the binding of ADP to the ATP site in the opposing subunit in the dimer, thus shifting the equilibrium for the phosphorylation of the second subunit to favor the hemiphosphorylated form of NRII under conditions where ADP is not removed. The results shown in Figure 1 suggest that this conformational change is temperature-dependent and thus slightly higher stoichiometry of NRII autophosphorylation was observed at lower temperature. The putative temperature-dependent conformational change probably also affects the stability of the doubly phosphorylated species in the absence of nucleotides (Figure 6).

The asymmetry of NRII autophosphorylation was not due to a kinetic barrier for phosphorylation of the second site in the dimer, but rather due to a difference in the equilibrium for the phosphorylation of the two subunits. The isotope exchange results observed in Figure 7B,C suggest that ADP was rapidly formed from ATP by phosphorylation of the small number of unphosphorylated sites in our NRII∼P_2 preparation. This suggests that the phosphorylation of the "second" sites in hemiphosphorylated species was rapid, but the reversal of this reaction was considerably more rapid.

Our experiments with heterodimers suggest that the asymmetry of NRII autophosphorylation was not preexisting but resulted from the autophosphorylation of the first subunit of the dimer. If the asymmetry was preexisting, we do not expect that the formation of heterodimers with unphosphorylatable NRII-H139N subunits should increrase the extent of NRII autophosphorylation, as it did (Figure 5).

Curiously, only a single phosphorylated species was detected when NRII∼P was subjected to nondenaturing gel electrophoresis (Figure 3). We have examined this issue extensively using a variety of electrophoretic conditions; in all cases results identical to those shown in Figure 3 were obtained. That is, we detected neither a species with intermediate mobility between unphosphorylated NRII and the species identified as NRII∼P nor a species with mobility greater than that of NRII∼P. These results suggest that only hemiphosphorylated NRII∼P was obtained after nondenaturing gel electrophoresis. Either fully phosphorylated NRII dimers became dephosphorylated to the hemiphosphorylated form soon after loading of these gels (for example, during migration through the stacking gel) or the doubly phosphorylated species had a mobility in these gels that is identical to that of the hemiphosphorylated form of NRII.

Previous results from Stock and colleagues (*22*), studying the CheA transmitter protein, indicated that the rate of phosphorylation of a small polypeptide containing the CheA site of autophosphorylation by a truncated CheA lacking this segment was considerably greater than the rate of autophosphorylation of intact CheA. That is, autophosphorylation was accelerated when the kinase activity and the phosphoaccepting site were on two different polypeptides. Furthermore, Stock and colleagues (*22*) showed that when heterodimers were formed between intact CheA and subunits of CheA lacking the phosphoaccepting site, these heterodimers phosphorylated the isolated phosphoaccepting polypeptide at a rate similar to that seen with intact CheA. Thus, the presence of a single phosphorylated site in CheA prevented the phosphorylation of the isolated phosphoaccepting polypeptide. However, the experiments by Stock and colleagues (*22*) were conducted in the presence of an enzymatic system for the removal of ADP; thus, the relationship of their observations to those reported here is unclear.

In cells, where the ADP concentration is roughly within an order of magnitude of the ATP concentration, we expect that NRII autophosphorylation will use only half of the available sites. Since the two-component system transmitter proteins are very similar, we expect that this should be true of the other transmitter proteins as well. In some cases, this may permit regulation of the extent of receiver phosphorylation by the energy charge of the cell. We observed that, at equilibrium, physiological levels of ADP had a significant effect on the levels of NRI-N phosphorylation (Figure 10). However, the low levels of ADP generated in the phosphorylation reactions did not seem to affect the extent or rate of NRI-N phosphorylation by NRII, suggesting that under these conditions, the formation and breakdown of the hemiphosphorylated form of NRII largely determined the rate and extent of NRI-N phosphorylation.

The PII signal transduction protein inhibited the rate of NRII autophosphorylation but slightly increased the extent of NRII autophosphorylation at equilibrium (Figure 9). PII may bind to the hemiphosphorylated form of NRII better than it binds to unphosphorylated NRII. We did not observe a significant effect of PK and PEP on the ability of PII to bring about the dephosphorylation of NRI-N by NRII. This

is probably because, in our reaction mixtures containing NRI-N and excess NRII, the hemiphosphorylated form of NRII was present regardless of whether PK and PEP were present. That is, the effect of NRI-N in dephosphorylating NRII could not be counteracted by addition of PK and PEP at the conditions used.

Why should such a curious mechanism of asymmetric autophosphorylation of the transmitter protein have been selected in evolution of the two-component signal transduction systems? One possibility is that the mechanism limits the rate of ATP consumption while rendering the system responsive to physiological ADP concentrations. Also, the hemiphosphorylated species may serve as the target for regulatory factors such as the PII protein. Finally, the conformational change that occurs upon phosphorylation of the first site within the NRII dimer may play an important role in making the phosphorylated His139 site available for transfer of the phosphoryl groups to the NRI receiver domain.

ACKNOWLEDGMENT

We thank Emmanuel S. Kamberov for sharing unpublished data regarding the nondenaturing gel electrophoresis technique and David P. Ballou for advice and stimulating discussions. We thank our colleagues Mariette R. Atkinson, Dr. Emmanuel S. Kamberov, Phyllis Zucker, Dr. Quan Sun, and Augen Pioszak for contributing purified proteins for this work.

REFERENCES

1. Ninfa, A. J. (1996) *Escherichia coli and Salmonella: Cellular and Molecular Biology* (Neidhardt, F. C., Ed.) pp 1246−1261, American Society for Microbiology Press, Washington, DC.
2. Parkinson, J. S., and Kofoid, E. C. (1992) *Annu. Rev. Genet. 26*, 71−112.
3. Stock, A. M., and Stock, J. B. (1987) *J. Bacteriol. 169*, 3301−3311.
4. Ninfa, A. J., and Magasanik, B. (1986) *Proc. Natl. Acad. Sci. U.S.A. 83*, 5909−5913.
5. Surette, M. G., Levit, M., Liu, Y., Lukat, G., Ninfa, E. G., Ninfa, A., and Stock, J. B. (1996) *J. Biol. Chem. 271*, 939−945.
6. Ninfa, A. J., and Bennett, R. L. (1991) *J. Biol. Chem. 266*, 6888−6893.
7. Hess, J. F., Oosawa, K., Kaplan, N., and Simon, M. I. (1988) *Cell 53*, 79−87.
8. Swanson, R. V., Schuster, S. C., and Simon, M. I. (1993) *Mol. Microbiol. 8*, 435−441.
9. Yang, Y., and Inouye, M. (1991) *Proc. Natl. Acad. Sci. U.S.A. 88*, 11057−11061.
10. Ninfa, E. G., Atkinson, M. R., Kamberov, E. S., and Ninfa, A. J. (1993) *J. Bacteriol. 175*, 7024−7032.
11. Weiss, V., and Magasanik, B. (1988) *Proc. Natl. Acad. Sci. U.S.A. 85*, 8919−8923.
12. Sanders, D. A., Gillece-Castro, B. L., Stock, A. M., Burlingame, A. L., and Koshland, D. E., Jr. (1989) *J. Biol. Chem. 264*, 21770−21778.
13. Stock, A. M., Wylie, D. C., Mottonen, J. M., Lupas, A. N., Ninfa, E. G., Ninfa, A. J., Schutt, C. E., and Stock, J. B. (1988) *Cold Spring Harbor Symp. Quant. Biol. 53* (Pt 1), 49−57.
14. Kamberov, E. S., Atkinson, M. R., Feng, J., Chandran, P., and Ninfa, A. J. (1994) *Cell. Mol. Biol. Res. 40*, 175−191.
15. Keener, J., and Kustu, S. (1988) *Proc. Natl. Acad. Sci. U.S.A. 85*, 4976−4980.
16. Jiang, P., and Ninfa, A. J. (1999) *J. Bacteriol. 181*, 1906−1911.
17. Kamberov, E. S., Atkinson, M. R., Chandran, P., and Ninfa, A. J. (1994) *J. Biol. Chem. 269*, 28294−28299.
18. Atkinson, M. R., and Ninfa, A. J. (1993) *J. Bacteriol. 175*, 7016−7023.
19. Lowry, O. H., Rosenbrough, N. J., Farr, A. L., and Randall, R. J. (1951) *J. Biol. Chem. 193*, 265−275.
20. Atkinson. M. R., Kamberov, E. S., Weiss, R. L., and Ninfa, A. J. (1994) *J. Biol. Chem. 269*, 28288−28293.
21. Jiang, P., Peliska, J. A., and Ninfa, A. J. (1998) *Biochemistry 37*, 12782−12794.
22. Levit, M., Liu, Y., Surette, M., and Stock, J. (1996) *J. Biol. Chem. 271*, 32057−32063.

BI992921W